古 脊 椎 动 物 学 报
VERTEBRATA PALASIATICA

A skull of *Machairodus horribilis* and new evidence for gigantism as a mode of mosaic evolution in machairodonts (Felidae, Carnivora)

DENG Tao[1,2,3] ZHANG Yun-Xiang[3] Zhijie J. TSENG[4] HOU Su-Kuan[1]

(1 *Key Laboratory of Vertebrate Evolution and Human Origins*, *Institute of Vertebrate Paleontology and Paleoanthropology*, *Chinese Academy of Sciences* Beijing 100044, China dengtao@ivpp.ac.cn)
(2 *CAS Center for Excellence in Tibetan Plateau Earth Sciences* Beijing 100101, China)
(3 *Department of Geology*, *Northwest University* Xi'an, Shaanxi 710069, China)
(4 *Division of Paleontology*, *American Museum of Natural History* New York, NY 10024, USA)

Abstract Sabertooth cats were extinct carnivorans that have attracted great attention and controversy because of their unique dental morphology representing an entirely extinct mode of feeding specialization. Some of them are lion-sized or tiger-sized carnivorans who are widely interpreted as hunters of larger and more powerful preys than those of their modern nonsaber-toothed relatives. We report the discovery of a large sabertooth cat skull of *Machairodus horribilis* from the Late Miocene of northwestern China. It shares some characteristics with derived sabertooth cats, but also is similar to extant pantherines in some cranial characters. A functional morphological analysis suggests that it differed from most other machairodont felids and had a limited gape to hunt smaller preys. Its anatomical features provide new evidence for the diversity of killing bites even within in the largest saber-toothed carnivorans and offer an additional mechanism for the mosaic evolution leading to functional and morphological diversity in sabertooth cats.

Key words Gansu, China; Late Miocene; sabertooth cat; skull; predatory behavior

1 Introduction

Sabertooth cats (Machairodontinae) were widely distributed in the Neogene and Quaternary faunas of the Old and New Worlds (Werdelin, 1996; McHenry et al., 2007). They were a long-living extinct clade among carnivorans, appearing from the Middle Miocene, and became extinct after a brief period of coexistence with early human beings in the Early Holocene (for example, at Rancho La Brea in Los Angeles, California, USA) (Turner and Antón, 1997). Some scenarios for the demise of the largest sabertooth cats include one where early human beings had gradually developed stronger hunting ability to outcompete the sabertooth cats, and/or sabertooth cats themselves becoming the prey of human beings (Martin, 1989). Like living big cats (Pantherinae), the large size of sabertooth cats is an advantage in predatory activity (Turner and Antón, 1997; Antón and Galobart, 1999; Andersson et al.,

国家自然科学基金重点项目(批准号：41430102)、国家重点基础研究发展计划项目(编号：2012CB821906)和中国科学院战略性先导科技专项(编号：XDB03020104)资助。
收稿日期：2015-11-06

2011; Salesa et al., 2005), and some of them had a lion-like or tiger-like size (adult body mass even more than 400 kg for *Smilodon populator*) (Christiansen and Harris, 2005; de Castro and Langer, 2008). On the other hand, the early materials of sabertooth cats were mostly fragmentary, therefore body size disparity and evolution throughout the machairodont felids are not well characterized. Only recently, several complete skulls of machaiodonts were described from Europe and China (Antón et al., 2004; Geraads et al., 2004; Qiu et al., 2008), among which *Machairodus horribilis* was considered to be the largest one (Qiu et al., 2008). The sizes of these machairodonts are judged according to their skulls with basilar lengths from 285 mm to 299 mm, and within this large-size class there are additional distinct morphological differences. Among them, some forms are similar to the highly specialized *Smilodon* and *Homotherium*, whereas others are more similar to extant pantherines. These important materials of sabertooth cats document mosaic evolution and the resulting significant morphological and ecological diversity in the evolutionary radiation of these carnivorans (Antón, 2013).

Here we report on a large sabertooth cat skull found to date from the Late Miocene *Hipparion* Red Clay at Longjiagou in Wudu County, Gansu Province, China, with the geographical coordinates of 33°35′N, 104°50′E (Zhang and Xue, 1995). The Longjiagou Basin is located on a planation surface of 2400-2600 m, which formed in the Late Miocene, and it is a small intramontane basin with an area of about 15 km^2, with lengths of about 6.5 km in north and south and 1–2.5 km in east and west. The fossiliferous bed is dark red silty mudstone, with blue-gray sandstones, lower part of which is mudstones with conglomerates, 20–340 m in total thickness. A comprehensive study about the Longjiagou *Hipparion* fauna is currently being carried out. From the present classification of the specimens, it shows that most elements of this fauna are typical fossil mammals of Baodean. Therefore biostratigraphically the fauna is almost certainly of Baodean age. However, the fauna includes younger faunal elements, for example, *Gazella* cf. *G. blacki*, which are found mainly in the Early Pliocene. *Hipparion platyodus* from Wudu is more derived than other Turolian *Hipparion* in other regions of China. As a result, the age of the Longjiagou fauna is tentatively assigned to late Baodean (Zhang and Xue, 1995; Qiu et al., 2013; Deng et al., 2013).

Institutional abbreviations Ath. Nr. fossil number of Museum of Palaeontology and Geology, University of Athens; HMV. vertebrate fossil number of Hezheng Paleozoological Museum; IVPP. Institute of Vertebrate Paleontology and Paleoanthropology, Chinese Academy of Sciences; LACM. Natural History Museum of Los Angeles County; NWU. Northwest University; V. vertebrate fossil number of IVPP.

2 Systematic paleontology

Order Carnivora Bowdich, 1821

Family Felidae Fischer, 1817

Subfamily Machairodontinae Gill, 1872

Genus *Machairodus* Kaup, 1833

***Machairodus horribilis* Schlosser, 1903**

(Figs. 1, 2; Tables 1, 2)

Referred material NWU 48Wd0001, an adult skull, laterally compressed (Figs. 1, 2). Because crushing has in all cases been lateral, measurements along the long axis of the skull are generally reliable, but overall width measurements are impossible to take in most cases (Table 1). Among its anterior dentition, only lower parts of both the right I3 and canine crowns are preserved. The zygomatic arches are lost. The right cheek teeth are relatively fragmentary, with a M1 root. The left P4 lacks its crown apices.

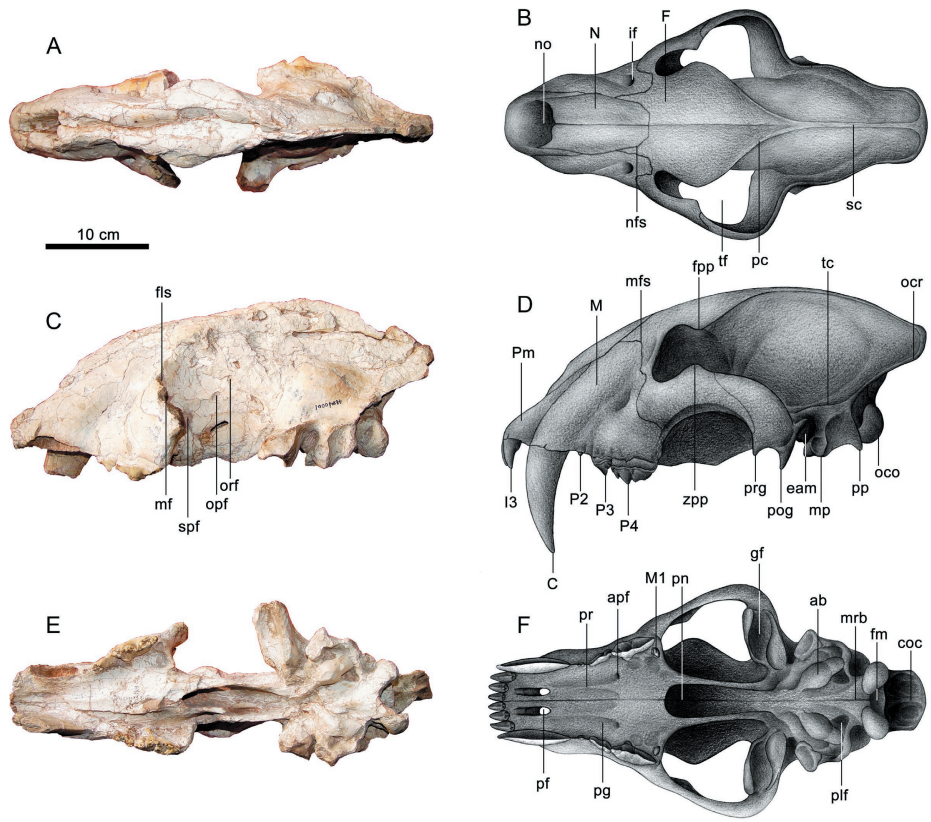

Fig. 1 Skull of *Machairodus horribilis* (NWU 48Wd0001) from Longjiagou (Wudu, Gansu Province, China)
A. dorsal view; B. reconstruction in dorsal view; C. lateral view; D. reconstruction in lateral view;
E. ventral view; F. reconstruction in ventral view

Abbreviations: ab. auditory bulla; apf. anterior palatine foramen; C. upper canine; coc. central occipital crest; eam. external auditory meatus; F. frontal bone; fls. fossa for lacrimal sac; fm. foramen magnum; fpp. frontal postorbital process; gf. glenoid fossa; I3. upper third incisor; if. infraorbital foramen; M. maxillary bone; M1. upper first molar; mf. maxillary foramen; mp. mastoid process; mrb. median ridge of the basioccipital; N. nasal bone; nfs. naso-frontal suture; no. nasal opening; oco. occipital condyle; ocr. occipital crest; opf. optic foramen; orf. orbital foramen; P2. upper second premolar; P3. upper third premolar; P4. upper fourth premolar; pc. parietal crest; pf. palatine fissure; pg. palatine groove; plf. posterior lacerated foramen; Pm. premaxillary bone; pn. posterior nares; pog. postglenoid process; pp. paroccipital process; pr. palatine ridge; prg. preglenoid process; sc. sagittal crest; spf. sphenopalatine foramen; tc. temporal crest; tf. temporal fossa; zpp. zygomatic postorbital process

Table 1 Selected measurements and comparison of the sabretooth cat specimens (mm)

	M. horribilis (male) NWU 48Wd0001	*M. horribilis* (female) V 15642 Qiu et al., 2008	*M. giganteus* Ath.Nr.1967/6 Melentis, 1968	*M. aphanistus* Maximum Antón et al., 2004	*S. fatalis* LACM 67/D817	*H. crenatidens* HMV 1213 Qiu et al., 2004	*M. nihowanensis* HMV 1220 Qiu et al., 2004
Vertex L	415	353	355	348*	356.5	330	265
Condylobasal L	370	318			325	305	
Basilar L	348	299	285	313.2	300	275	242
Palatal L	163	163	160	146*	151	~142	118
Width at I3	~63	60		48*	54	58*	
Width at C-C	~100	90	64	71*	98	>65	70
Width behind P4	134	138	104	92*	134	108*	
Width at postorbital process	~120	132	118	96*	115		
Occipital H	124	120		123*	104.5	94*	
Width at mastoid process	~136	127	128	113	135		
H at mastoid process	~163	142	122	117*	149	124*	
I3 L×W	17×15	12.6×11			19×12		
C1 L×W	48.4×18.4	39.5×16	35.2×14.3	35.7×14.5	36.7×16.7	30.2×13.5	27.5×14
P3 L×W	26.6×12	24.3×9.6	23.7×10.6	23.7×12	19.8×9		12.2×6
P4 L×W	43×17	42.2×15	43.1×14.8	36.4×17.4	44.4×16.7	44.8×14	33.7×13.7

*Measured from figures.

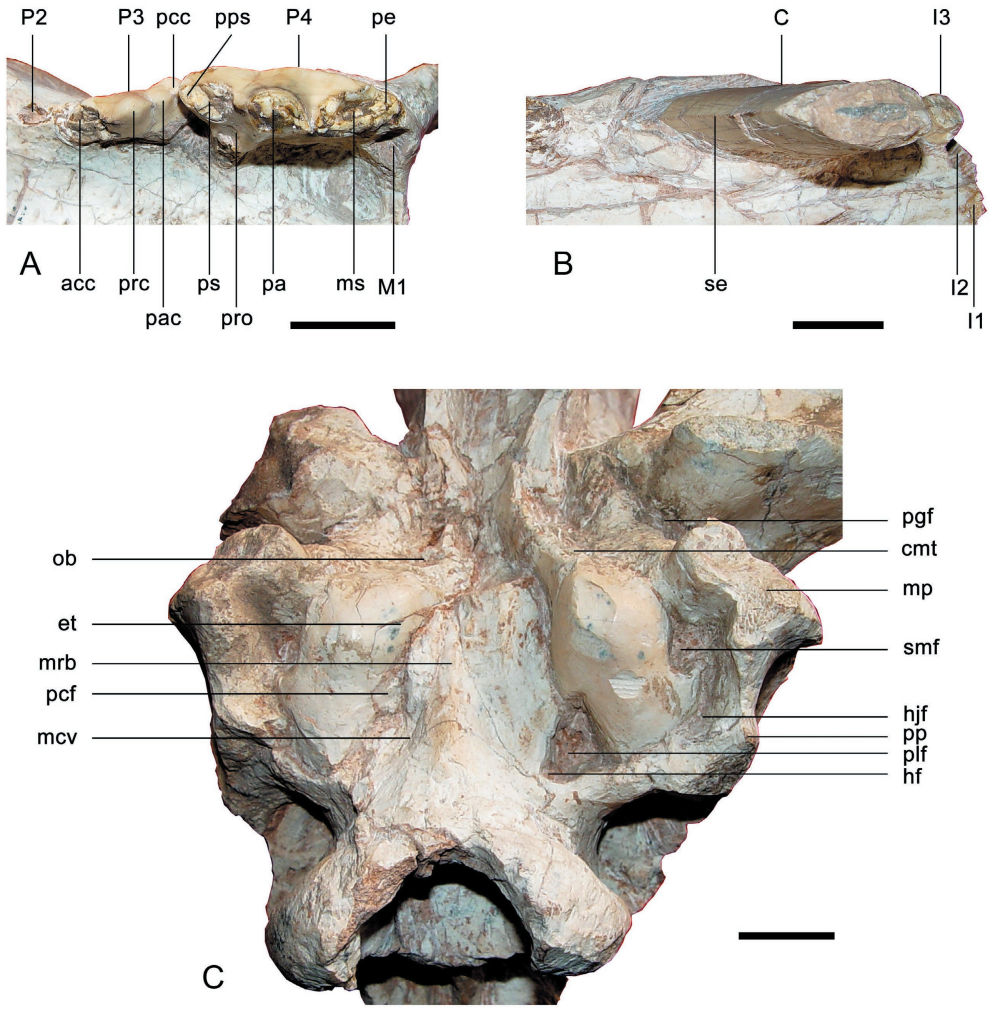

Fig. 2 Teeth and basioccipital region of *Machairodus horribilis* (NWU 48Wd0001)
A. upper cheek teeth in occlusal view; B. upper anterior teeth in occlusal view;
C. basioccipital region in ventral view

Abbreviations: acc. anterior cingular cusp; C. upper canine; cmt. canalis musculotubarius; et. entotympanics; hf. hypoglossal foramen; hjf. hyojugular fossa; I1. upper first incisor; I2. upper second incisor; I3. upper third incisor; M1. upper first molar; mcv. attachment area for musculus rectus capitis ventralis; mp. mastoid process; mrb. median ridge of the basioccipital; ms. metastyle; ob. antero-medial opening of bulla; P2. upper second premolar; P3. upper third premolar; P4. upper fourth premolar; pa. paracone; pac. posterior accessory cusp; pcc. posterior cingular cusp; pcf. doubled posterior carotid foramen; pe. posterior edge; pgf. postglenoid foramen; plf. posterior lacerated foramen; pp. paroccipital process; pps. pre-parastyle; prc. principal cusp; pro. protocone; ps. parastyle; se. serration; smf. stylomastoid foramen. Scale bars equal 2 cm

Locality and horizon Longjiagou Town, Wudu County, Gansu Province in northwestern China; Late Miocene *Hipparion* Red Clay.

Description and comparisons NWU 48Wd0001 represents an adult individual, given by the eruption and wear of the teeth and the fusion of the bone sutures. With a cranial vertex

length of 415 cm, this skull obviously exceeds the length of all known Late Miocene skull specimens of sabertooth cats, including other *Machairodus horribilis* (353 mm, V 15642) and also *M. giganteus* (355 mm, Ath. Nr. 1967/6). This skull most likely represents an adult male of *M. horribilis* (Table 2).

In dorsal view (Fig. 1A, B), two nasal bones compose a hexagon that is longer than wide, and whose antero-posterior mid-points are projected laterally, rather than narrowing posteriorly as in pantherines (Antón et al., 2004). The posterior half of the naso-frontal suture is perpendicular to the sagittal axis of the skull, and the sagittal process of the frontal is absent, but the lateral process, which inserts into the nasal and maxillary bones, is marked, with a length of 22.5 mm. The temporal fossa is antero-posteriorly elongated, which occurs consistently in some primitive sabertooth cats (Salesa et al., 2005). The dorsal outline of the frontal region at the level of the postorbital processes is concave, which is similar to those of some primitive sabertooth cats. The shape of the nasal opening is intermediate between the heart-shaped outline observed in pantherines and the rectangular shape typical of more derived machairodontines like *Homotherium* and *Smilodon* (Antón et al., 2004). The frontal bone is wide and penetrated deeply into the maxilla, which is similar to primitive sabertooth cats; its postorbital process is strong and thick to form a low and short triangular pyramid, without a sharp tip, and with a large rough surface that extend both anteriorly and posteriorly, which is similar to derived sabertooth cats (Qiu et al., 2004). The parietal crests converge into a single sagittal crest at the level of the external auditory meatus, and anterior to the convergent point is a weak sagittal groove, unlike the obvious depression at this position in *M. aphanistus* (Antón et al., 2004). The muzzle may be narrower at the level of the canine alveoli than that of the lion, due in part to the much more flattened section of the upper canines.

Table 2 Index of sexual dimorphism (male measurement value: female measurement value) for *Machairodus horribilis* and several other felid species

	NWU 48Wd0001: IVPP V 15642	IVPP V 15643: IVPP V 15642	*Machairodus aphanistus* Antón et al., 2004	*Smilodon fatalis* Van Valkenburgh and Sacco, 2002	*Panthera leo* Antón et al., 2004
Vertex L	1.18				
Condylobasal L	1.16		1.24	1.06	1.12
Basilar L	1.16				
Palatal L	1.00				
I3 L	1.36	1.37			
I3 W	1.35	1.29			
C L	1.23	1.12	1.22	1.09	1.25
C W	1.15	1.26	1.16	1.12	1.23
P3 L	1.09	0.99			
P3 W	1.25	1.00			
P4 L	1.02	1.11			
P4 W	1.13	1.31			

In lateral view (Fig. 1C, D), the dorsal profile is about as convex as in the lion, but different from the straighter dorsal profiles in more derived machairodontines (Antón et al., 2004). The occipital plane has a great inclination, which is exhibited in some primitive

sabertooth cats (Salesa et al., 2005). The alveolus region of incisors is not strongly projected forward so that the antero-dorsal margin of the premaxillary bone is weakly curved and declined. The infraorbital foramen is large and rounded, which is similar to those of derived sabertooth cats in shape and size, and its posterior border is located above the parastyle of P4. The sagittal crest rapidly becomes high as a vertical plate with a maximum depth of about 58 mm, which is the most striking difference from living pantherine cats. The postglenoid and mastoid processes are widely separated (8.5 mm), especially on their distal ends, so that the external auditory meatus is not closed as in pantherines, the external auditory meatus is not enclosed between the postglenoid and mastoid processes. The mastoid process is robust and strongly extends inferiorly, covering the auditory bulla laterally. The mastoid and the paroccipital processes are also widely separated, but connected by a wide curved edge.

In ventral view (Fig. 1E, F), the diastema between I3 and C is 12 mm, slightly shorter than the length of I3 (15 mm), and its labial margin is weakly concave, so the alveolus margins of the incisors and canine are obviously separated. The palate is sunken below the cheek teeth so that their roots are exposed. There is a pair of projecting ridges that extend from the postero-medial corner of the palatine fissure to the medial side of the anterior palatine foramen as the medial boundary of the palatine groove, with a premaxillary section which is markedly crest-like, becoming more blunt in the maxillary and even more so in the palatine. The well-developed palatine ridge is related to the gripping device (Antón and Galobart, 1999). The posterior margin of the palate is U-shaped, without a sagittal process and a marked sagittal indentation seen in pantherines, and its bottom is located at the level of M1. Because the skull is compressed laterally, the original shape of the posterior nares cannot be known.

The median ridge of the basioccipital extends anteriorly to reach the level of the anterior end of the auditory bullae, which is similar to those of derived sabertooth cats. The posterior half of the basioccipital part is a convex triangle, and smoothly connects with the occipital condyles; the central crest is not very strong, and both sides are deep depressions for the insertion of the rectus capitis anticus major muscle, whose anterior tip disappears between a pair of rough swellings in attachment for the rectus capitis ventralis muscle (Fig. 2), which is more anteriorly than in pantherines. Although the terminal of the postglenoid process is broken, it is still judged to strongly extend ventrally, so the posterior surface of the glenoid fossa is almost vertical. The preglenoid process is well developed and laterally located, being different from the crest-like anterior border in more derived machairodontines (Christiansen, 2013). As a result, the glenoid fossa is very deep as in the modern lion and leopard, suggesting comparable ranges of jaw motion in *M. horribilis*. In ventral view, the fossa is elongated as in pantherines, rather than widening medially as in derived sabertooth cats. The space between the postglenoid and mastoid processes is broad, which is similar to that of pantherines, but not as in later machairodontines, where both processes tend to come ever closer to each other, almost touching in *Smilodon* (Antón et al., 2004). The temporal crest is more developed than in pantherines and weaker than in later machairodontines. The mastoid process is especially

robust and located at the anterior 3/4 of the auditory bulla, with a laterally flaring mastoid crest as in derived sabertooth cats. The insertion of the atlantomastoid muscles, which is located under this crest, is thus enlarged, and it becomes oriented more inferiorly and less laterally than in pantherines (Antón et al., 2004). The paroccipital process is located near the postero-lateral end of the auditory bulla, with a long distance from the mastoid process, which equals to the distance from the occipital condyle.

In occipital view, the occipital surface is a high triangle with a pair of laterally projecting processes near its top, and the occipital crest also surrounds a triangle on the top of the occipital surface, as in pantherines. The central smooth region is divided into two pairs of depressions: one is located laterally to the occipital condyle, and the other is located superiorly to the occipital condyle. Below the top margin and on the each side of the central crest, there are deep depressions for the attachment of muscles, which are absent in pantherines. Lateral to the upper margin of the foramen magnum there is a pair of vertical edge-like processes, weaker than tubercles at the same position in pantherines.

The incisors are arranged in gentle arch, instead of a highly curved arrangement in more derived machairodontines, but those teeth exhibit several rudimentary characteristics that are better developed in derived machairodontines (Qiu et al., 2004). Judged from the alveolus, the incisors are enlarged from I1 to I3 gradually, but I3 is obviously much larger and more robust, with a weak antero-lingual edge and a sharp postero-labial edge, and without serration when it is worn. The smaller first and second incisors and the larger third incisor set in a slight arch, only slightly more developed than the straight incisor rows of the primitive sabertooth cats (Christiansen, 2013).

Both the anterior and posterior margins of the huge upper canine of *M. horribilis* are serrated, with higher height in the posterior edge (Fig. 2B), similar to the serration seen in other sabertooth cats, such as *Homotherium* (Qiu et al., 2004). The upper canine is large and long, with an antero-posterior basal length of 48.4 mm and a thickness of 18.4 mm. The labial swelling of the crown is slightly stronger than the lingual one, and the cross section of the crown is wider in the anterior end than in the posterior end.

P2's alveolus has a length of 8 mm and a width of 4.5 mm, with a single root, as in pantherines. The diastema is 7 mm between P2 and C and about 4 mm between P2 and P3. P3 has double roots, a principal cusp, a posterior accessory cusp, and a posterior cingular cusp (Fig. 2A), the latter is absent in both *Panthera leo* and *M. giganteus*. The labial border is straight in the middle and anterior parts, but curved labially at the posterior part, whereas in *P. leo* and *M. giganteus* that border is straight; the lingual border is slightly concave in the middle and curved labially in the posterior, whereas it is projecting lingually in *M. aphanistus* (Antón et al., 2004). There is a broken scar at the lingual base between the principal and posterior accessory cusps, which is seem to indicate a prominence in its original state. Both the anterior and posterior edges of the principal cusp are serrated. The posterior accessory cusp is much lower than the principal cusp, and the posterior cingular cusp is also much lower than the posterior accessory

cusp.

P4 has a pre-parastyle and a very rudimental protocone supported by an independent root (Fig. 2A). This carnassial tooth has complete enamel to cover its crown, except for the broken cusps' apices. In the crown base, there is a V-shaped groove between the antero-labial root and the protocone root. There is a marked depression in front of the protocone, and the crown part of the protocone is a weak swelling on the lingual wall, instead of an isolated cone, similar to the condition seen in derived sabertooth cats (Qiu et al., 2004). In comparison, *M. aphanistus* has a well-developed protocone (Antón et al., 2004). Among the extant felids, the protocone is well developed in all species except in the cheetah, *Acinonyx jubatus* (Ficcarelli, 1984). At the base of the labial wall of the pre-parastyle, there are three tiny granular tubercles. On the posterior part of the labial wall of the metastyle, there is a projecting edge oblique posteriorly.

The root indicates that M1 is located in the lingual side of the posterior end of P4 (Fig. 1). It is oval in shape with a labial-lingual diameter of 8.7 mm and an antero-posterior diameter of 7 mm, longer but narrower than that of *M. palanderi* and other known *M. horribilis* (Qiu et al., 2008).

3 Body weight estimation of *Machairodus horribilis*

In order to determine the body mass of *Machairodus horribilis*, we utilized allometric equations relating weight with skull measurements to estimate body mass. Body mass is an ecologically relevant characteristic like life history traits, diet, population density, population growth rate, home range size, and behavioral adaptations. In fact, based upon modern knowledge, a mammal's body size may be the most useful single predictor of that species' adaptations (Damuth and MacFadden, 1990).

An entire book (Damuth and MacFadden, 1990) has been written on the challenges associated with estimating body weights from mammalian osteological remains. Least squares regression of $\log_{10}$ transformed data is used to model the association between body mass and skeleton. The regression of log body weight (W) against log condylobasal length (CBL) for Felidae (Van Valkenburgh, 1990) is chosen to calculate the body weight of *M. horribilis*:

$$log\ W = 3.11 log\ CBL - 5.38$$

The correlation coefficient (r) of condylobasal length and body weight is high (0.92). The percent prediction error (%PE) is 38, and the percent standard error of the estimate (%SEE) is 57.

According to the size of the skull (NWU 48Wd0001, Table 1), *M. horribilis* from Longjiagou is estimated to have had a body weight of about 405 kg as a living animal.

4 Phylogenetic analysis

In order to investigate the phylogenetic position of the newly described specimen of *M. horribilis* (NWU 48Wd0001), we added this specimen and the material of *M. horribilis* described by Qiu et al. (2008) to a recently published comprehensive dataset on sabertooth cat

phylogeny (Christiansen, 2013:appendix 3) to confirm their Machairodontine affinities (Table 3). Scorings for *M. horribilis* from Longjiagou were based on the skull (NWU 48Wd0001) and for *M. horribilis* from Baode were based on skull and mandible (IVPP V 15642). We removed *Dinictis* from the data matrix because of the problematic phylogenetic position of nimravids highlighted by recent cladistics analyses of Carnivoramorpha employing postcranial characters (Spaulding and Flynn, 2012). However, *Canis lupus* and *Cryptoprocta ferox* were retained as caniform and feliform outgroups, respectively. The data matrix was analysed using the TNT software package (Goloboff et al., 2008) and PAUP* (Swofford, 1991). Analyses in TNT were run using both implicit enumeration and traditional search, with default settings apart from the following: 99999 maximum trees in memory and 1000 replications. The analysis resulted in 19 equally parsimonious trees, each having a length of 116 steps, a CI of 0.621, and a RI of 0.805. Analyses in PAUP* were run with the heuristic search option with all default settings except for NREPS set to 1000 replications. The analysis resulted in 65 equally parsimonious trees, each having a length of 116 steps, a CI of 0.638, and a RI of 0.829. Both TNT and PAUP* produced cladograms of identical topologies. We next estimated support for the clades present in the strict consensus tree by running bootstrap and jackknife resampling analyses in both programs with 1000 replications. In addition, we calculated decay index (or Bremer support) in both programs. We also calculated support values using the symmetric resampling function in TNT. Lastly, we analyzed the dataset under a Bayesian framework using MrBayes version 3.2 (Ronquist et al., 2012). The morphology matrix was treated as a single partition assigned with the Mk model for morphology. The analyses were run for 10 million generations with 8 simultaneous chains, sampling every 1000 trees. The strict consensus tree is shown in Fig. 3, with support values indicated for the major clades.

Table 3 Character codes of *Machairodus horribilis* according to Christiansen (2013, appendix 3)

Character	1 1234567890	1111111112 1234567890	2222222223 1234567890	3333333334 1234567890	4444444445 1234567890
A. horribilis (IVPP V 15642)	1220121111	2110111121	1110011111	1101311011	1111011011
A. horribilis (NWU 48Wd0001)	122?121111	2110111112?	??????????1	1101311021	11?10?????

The unambiguous synapomorphies for the monophyletic sabertooth cats (Machairodontinae): small c1, very small knob-like M1, and a large P3 parastyle (Christiansen, 2013) are seen in both specimens of *M. horribilis*. The analysis of the sabertooth cat dataset place *M. horribilis* and *M. giganteus* as unresolved taxa at the base of a weakly supported Homotherini + *Smilodon* clade. The basal position of *M. aphanistus* and more crownward placement of *M. giganteus* and *M. horribilis* in the consensus tree are consistent with the result of Christiansen (2013). Because *M. aphanistus* and *M. giganteus* do not form a monophyletic group in the consensus tree, Christiansen (2013) used the genus name *Amphimachairodus* proposed previously by Kretzoi (1929) for the latter species. On the other hand, we consider that some scorings of Christiansen (2013) are needed to check personally by ourselves in future, so the genus name *Machairodus* is still retained for these species tentatively.

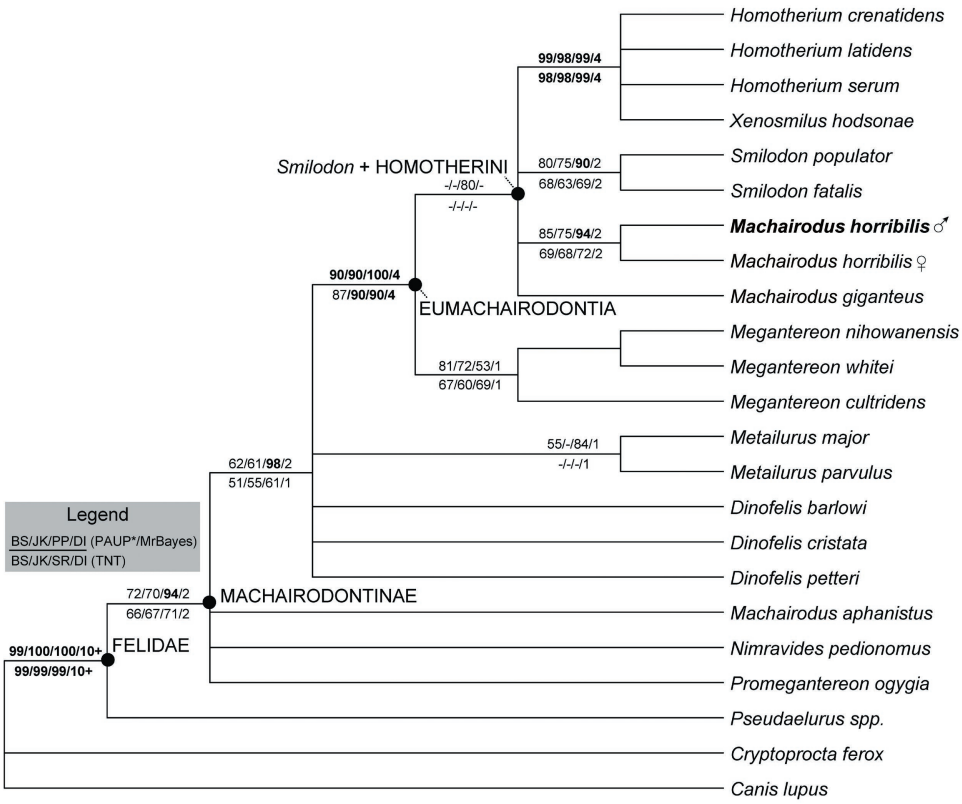

Fig. 3 A strict-consensus tree of sabretooth felids

The same topology was recovered in PAUP* (MPT=65, 116 steps, CI=0.638, RI=0.829) and TNT (MPT=19, 116 steps, CI=0.621, RI=0.805) analyses. Clade stability and support values from Bootstrap (BS, n=1000), jackknife (JK, n=1000), symmetric resampling (SR, n=1000), and decay index (DI) analyses are indicated. In addition, posterior probabilities from a Bayesian analysis of the morphological characters under the Mk model are provided. The base matrix was taken from Christiansen (2013:appendix 3) with the addition of *Machairodus horribilis* from Baode (female) and Wudu (male). Highly supported (support>90% and DI>=4) clades are indicated in bold. Position of specimen described in this study is also indicated in bold

5 Predatory behavior

A phylogenetic analysis places this specimen among the Eumachairodontia clade, and allied with other homotherins (Fig. 3). In combination with other recent discoveries, such as those of smaller, presumably female individuals of *M. horribilis* from the Late Miocene of Baode in Shanxi Province, China (Table 2; Qiu et al., 2008), the new find indicates that these machairodonts likely relied on unspecialized throat bites (Turner and Antón, 1997) in the Late Miocene woodland or steppe of the northwestern China to subdue their prey, but nevertheless with enough clearance between their upper and lower canines to prey on the most common contemporaneous ungulates, permitted by their gigantic size.

Gigantism affects many aspects of animal structure and function (Xu et al., 2012). Among living meat eaters, almost all species larger than about 21 kg prey on species as large or larger

than themselves because of energetic demands (Carbone et al., 1999). Because sabertooth cats were generally strongly built animals, it has been suggested that they specialized in taking larger prey than extant pantherines (Akersten, 1985; Turner and Antón, 1997). Differences among carnivoran species in killing and feeding behavior are often reflected in their craniodental morphology (Biknevicius et al., 1996). It was even once proposed that saber-like teeth evolved convergently in saber-toothed mammals and allosaurid dinosaurs as an adaptation for predation on prey species ten or more times heavier than the predators (Bakker, 1998). Larger predators specialize on larger prey (Radloff and du Toit, 2004). Given these observations and interpretations, does the gigantic body size of *M. horribilis* indicate that it must hunt very large preys, or does it account for a unique killing mechanism?

Indeed, there are several features indicating that *M. horribilis* killed its prey by penetrating the flesh of the throat with its canines and causing massive blood loss, just as has been inferred for the derived sabertooth cats (Turner and Antón, 1997; Wroe et al., 2005; McHenry et al., 2007). These features include the high crowned, flattened and serrated upper canines, which are well adapted to penetrate the flesh of prey and would be less suitable for either a crushing nape bite or a suffocating bite (Bryant and Churcher, 1987); the enlarged mastoid crests, slight anteroposterior projection of the mastoid process, and median crest on the basicranium indicate locations of muscle insertions consistent with adaptations for a canine shear-bite (Antón et al., 2004). The elongated and inclined occipital region further allows the movement of the temporalis to scribe a larger arc as the jaw closes, increasing the force generated at the anterior teeth (incisors and canines) rather than at the carnassials (Martin et al., 1999).

On the other hand, significant differences that exist among the various taxa of saber-toothed carnivorous mammals have been suggested to correlate with behavioral and ecological diversity (Martin, 1980; Bryant and Churcher, 1987, Turner and Antón, 1997; Martin et al., 1999). If a throat bite was the main killing technique of sabertooth cats, then killing of a larger prey required a larger gape. For example, *Smilodon* has an enormous gape of 120° (Antón et al., 2004; Andersson et al., 2011). On the other hand, *M. horribilis* has the strong pre- and postglenoid processes to make its glenoid fossa very deep, which is similar to the pantherine, such as the lion and leopard, so it has only a moderate gape of about 70° (Antón et al., 1998; Andersson et al., 2011). Moreover, the inclined occiput of *M. horribilis* indicates that the fibers of the temporal muscle are strongly inclined as in primitive cats, while in derived machairodontines these fibers become more vertically oriented (Antón et al., 2004). The larger degree of inclination in *M. horribilis* represents a limitation for dorsal extension of the head over the atlas, therefore in turn limits the head action required in the canine-shear bite (Antón et al., 2004; McHenry et al., 2007; but see recent discussion of *Smilodon* mechanism by Brown, 2014). Although the strongly developed mastoid crest of *M. horribilis* provides a larger area for insertion of the atlanto-mastoid muscles and indicates that the strength of these muscles would be greater than in pantherines, contributing to the potential for head depression, it is less efficient than in more derived machairodontines (Antón et al., 2004).

As a result, the functional morphology suggests that the biting or killing mechanism of *M. horribilis* differs from more highly specialized sabertooth cats, but in ways similar to that of extant lions and leopards and primitive, early felids. Specifically, the limited gape and the intermediate development of musculature arrangements compared to more derived sabertooth cats would have restricted *M. horribilis* to somewhat smaller prey sizes than more derived sabertooth cats with larger gapes. However, given its gigantic size, which effectively increases the absolute distance between upper and lower canines at maximum gape (assuming canine length scales proportionally to gape), *M. horribilis* nevertheless achieved some functionality of the sabers in biting and killing that is more specialized than less derived machairodontines such as *M. aphanistus* but not yet at the stage of derived homotherins such as *Homotherium*.

The highly mosaic evolution of sabertooth cats exhibits increasingly refined adaptations for the canine-shear bite in order to kill its prey with more efficiency. Efficiency is important because the ability to kill prey faster translates to less struggling time and less opportunity for accidents involving teeth breakage and/or prey escape (Van Valkenburgh, 1988; Van Valkenburgh and Ruff, 1987). The canines (length × width = 48.4×18.4 mm, index=2.63) of *M. horribilis* are at least as flattened as those of *M. giganteus* and *M. aphanistus* (Antón et al., 2004:table 3), and thus equally fragile and breakable (Van Valkenburgh, 1988; Van Valkenburgh and Ruff, 1987). Like hyaenids, the robust incisors, especially I3, and the less parabolic incisor arcade of *M. horribilis* may function to reinforce the adjacent canines during the killing bites by helping locally to limit the motion of the prey (Biknevicius et al, 1996).

The morphological features discussed above suggest a model of predatory behavior of *M. horribilis* that differs not only from that of extant pantherines but also from that hypothesized for derived machairodontines such as *Homotherium* and *Smilodon*. Faunal evidence for a great number of slow-running three-toed horses in the Longjiagou fauna that belong to a dwarf species *Hipparion platyodus* with very short limb bones (Qiu et al., 1987; Zhang and Xue, 1995) provides at least one candidate species as the possible principal prey of *M. horribilis*. Although also present in this fauna (Zhang and Xue, 1995), the deer *Eostyloceros* and *Cervavitus* may have been too small and too fast for *M. horribilis*, and the giraffes *Samotherium* and *Honanotherium* may have been too large for the felid predators.

The mosaic combination of highly derived upper canines and primitive cranial morphology in *M. horribilis* demonstrates that even though high-crowned, flattened sabers may work best as part of a complex of adaptations for the canine-shear bite, they can also work, and do work sufficiently well, within a different, more feline like mode of biting when combined with gigantic size. The key advantage of the initial development of saber-like teeth would lie in the efficiency of a killing bite that caused massive blood loss instead of suffocation, rather than in the possibility of taking significantly larger prey (Turner and Antón, 1997). It is reasonable, however, that more derived sabertooth cats with a larger gape and more specialized musculoskeletal complex than *M. horribilis* would have been able to take prey larger relative to their body size. The extent of gigantism as a beneficial addition to a mosaic

mode of improving sabertooth functionality may have been limited in sabertooth cat evolution given the relatively short stratigraphic range in which very large-bodied *Machairodus* occur.

This discovery has implications for early predatory behavior evolution of sabertooth cats, and indicates that at least one sabertooth cat incorporated gigantic size in the functional mosaic of musculoskeletal features associated with the sabertooth bite. The unique combination of a restricted gape and very large size in *M. horribilis* could represent an adaptation to a particular prey size class, given the multitude of paleoenvironments it has been found in. *M. horribilis* lived both in woodlands of Longjiagou and also in completely open grasslands (for example in Baode). As such *M. horribilis* likely was sympatric with forest mammals such as primates (Xue and Delson, 1989), chalicotheres (Xue and Coombs, 1985), and the deer *Eostyloceros* (Zhang and Xue, 1995) as well as more typical open grassland forms. The dwarf horses of the Longjiagou fauna are morphologically different from the tall *Hipparion* horses in Baode and other regions, in having a less cursorial postcranial skeleton that may have provided stable food supply for the population containing the largest known *Machairodus*. Different from the rich giraffids in other localities, the giraffids were rare for individuals and low in taxonomic diversity at Longjiagou. The predatory behavior of large carnivorans may be interpreted according to the mass-energetics "law" (Carbone et al, 1999), but the encounter rate for prey is also an important factor. Moreover, the height of giraffe increased its predator detection capability and threat of injury to predators from its hooves, thus it is not very suitable as a regular prey of sabertooth cats (Hayward and Kerley, 2005). Gigantic Late Miocene sabertooth cats elsewhere, by contrast, lived in an open steppe that was conducive for them to pursue preys at a burst of high speed and attack preys with a very large gape.

In conclusion, *M. horribilis* from Longjiagou has the largest skull of any sabertooth cat, but it likely did not exhibit the predatory behavior of derived taxa such as *Smilodon* or *Homotherium*, and instead hunted comparatively smaller preys. Derived predatory behaviors apparently have evolved several times independently in sabertooth cats along with changes of habitats and preys through the whole evolutionary history of sabertooth cats (Antón, 2013), as has clearly occurred in some ungulates, especially tooth crown changes in the family Equidae (Mihlbachler et al., 2011). The mixture of primitive and derived morphological characteristics in the cranium of *M. horribilis* is consistent with previously observed mosaic evolutionary patterns in early machairodontines, and additionally provides evidence that gigantism may be one of several mechanisms to increase gape prior to the evolution of the full suite of anatomical features associated with more efficient killing bite mechanism (Antón, 2013). Future discoveries of postcranial elements belonging to *M. horribilis* would allow these functional morphological interpretations to be further tested.

Acknowledgments We thank Prof. Xue Xiang-Xu for her contribution to the collection of the Longjiagou fauna, and Chen Yu for his illustrations of this specimen. This work was supported by the National Natural Science Foundation of China (41430102), the Strategic Priority

Research Program of the Chinese Academy of Sciences (XDB03020104), and the Ministry of Science and Technology of China (2012CB821906).

记恐剑齿虎一头骨及剑齿虎镶嵌进化中体型巨大化的新证据

邓 涛[1,2,3] 张云翔[3] 曾志杰[4] 侯素宽[1]

(1中国科学院古脊椎动物与古人类研究所，中国科学院脊椎动物演化与人类起源重点实验室 北京 100044)

(2中国科学院青藏高原地球科学卓越创新中心 北京 100101)

(3西北大学地质系 西安 710069)

(4美国自然历史博物馆古生物部 纽约 NY 10024)

摘要：剑齿虎是一类绝灭的食肉目动物，由于其独特的牙齿形态代表了已完全消失的特化取食方式而引起了极大的关注和争论。一些剑齿虎是狮子体型或老虎体型的食肉动物，它们被广泛认为能够比其不具剑形犬齿的现代近亲捕杀更大和更强壮的猎物。本文报道在甘肃省晚中新世地层中发现的一具属于恐剑齿虎(*Machairodus horribilis*)的大型头骨。这件标本的一些特征与进步的剑齿虎相同，但在某些头骨性状上则与现生的豹亚科种类相似。不同于其他大多数剑齿虎，功能形态分析指示该剑齿虎的口部张开程度受到限制，因此只能捕猎相对较小的猎物。这具头骨的解剖特征为证明即使在最大的具剑形犬齿的食肉目动物中也存在捕猎咬杀方式的多样性提供了新的证据，并揭示了在剑齿虎中导致功能和形态多样性镶嵌进化的另一种机制。

关键词：甘肃，晚中新世，剑齿虎，头骨，捕猎行为

References

Akersten W, 1985. Canine function in *Smilodon* (Mammalia, Felidae, Machairodontinae). Los Angeles Co Mus Contr Sci, 356: 1–22

Andersson K, Norman D, Werdelin L, 2011. Sabertoothed carnivores and the killing of large prey. Plos One, 6 (10): e24971. doi:10.1371/journal.pone.0024971

Antón M, 2013. Sabertooth. Bloomington and Indianapolis: Indiana University Press. 1–243

Antón M, Galobart A, 1999. Neck function and predatory behaviour in the scimitar toothed cat *Homotherium latidens* (Owen). J Vert Paleont, 19: 771–784

Antón M, García-Perea R, Turner A, 1998. Reconstructed facial appearance of the Sabretoothed felid *Smilodon*. Zool J Linnean Soc, 124: 369–386

Antón M, Salesa M J, Morales J et al., 2004. First known complete skulls of the scimitar-toothed cat *Machairodus aphanistus* (Felidae, Carnivora) from the Spanish Late Miocene site of Batallones-1. J Vert Paleont, 24: 957–969

Bakker R T, 1998. Brontosaur killers: Late Jurassic allosaurids as sabertooth cat analogues. Gaia, 15: 145–158

Biknevicius A R, Van Valkenburgh B, Walker J, 1996. Incisor size and shape: implications for feeding behaviors in saber-

toothed “cats”. J Vert Paleont, 16: 510–521

Brown J G, 2014. Jaw function in *Smilodon fatalis*: a reevaluation of the canine shear-bite and a proposal for a new forelimb-powered class 1 lever model. Plos One, doi: 10.1371/journal.pone.0107456

Bryant H N, Churcher C S, 1987. All sabertoothed carnivores aren’t sharks. Nature, 325: 488

Carbone C, Mace G M, Roberts S C et al., 1999. Energetic constraints on the diet of terrestrial carnivores. Nature, 402: 286-288

Christiansen P, 2013. Phylogeny of the sabertoothed felids (Carnivora: Felidae: Machairodontinae). Cladistics, 29: 543-559

Christiansen P, Harris J M, 2005. Body size of *Smilodon* (Mammalia: Felidae). J Morphol, 266: 369–384

Damuth J, MacFadden B J, 1990. Body Size in Mammalian Paleobiology: Estimation and Biological Implication. Cambridge: Cambridge University Press. 1–397

de Castro M C, Langer M C, 2008. New postcranial remains of *Smilodon populator* Lund, 1842 from South-Central Brazil. Rev Bras Paleont, 11: 199–206

Deng T, Qiu Z X, Wang B Y et al., 2013. Late Cenozoic biostratigraphy of the Linxia Basin, northwestern China. In: Wang X M, Flynn L J, Fortelius M eds. Fossil Mammals of Asia: Neogene Biostratigraphy and Chronology. New York: Columbia University Press. 243-273

Ficcarelli G, 1984. The Villafranchian cheetahs from Tuscany and remarks on the dispersal and evolution of the genus *Acinonyx*. Palaeont Ital, 73: 94–103

Geraads D, Kaya T, Tuna V, 2004. A skull of *Machairodus giganteus* (Felidae, Mammalia) from the Late Miocene of Turkey. N Jahrb Geol Paläontol Mh, 2: 95–110

Goloboff P A, Farris J S, Nixon K C, 2008. TNT, a free program for phylogenetic analysis. Cladistics, 24: 774–786

Hayward M W, Kerley G I H, 2005. Prey preferences of the lion (*Panthera leo*). J Zool, 267: 309–322

Kretzoi M, 1929. Materialen zur phylogenetischen Klassifikation der Aeluroïden. 10th Int Zool Congr, 2: 1293–1355

Martin L D, 1980. Functional morphology and the evolution of cats. Trans Nebraska Acad Sci, 8: 141–154

Martin L D, Babiarz J P, Naples V L et al., 1999. Three ways to be a sabertoothed cat. Naturwissenschaften, 87: 41–44

Martin P S, 1989. Prehistoric overkill: a global model. In: Martin P S, Klein R G eds. Quaternary Extinctions: A Prehistoric Revolution. Tucson: The University of Arizona Press. 354–404.

McHenry C R, Wroe S, Clausen P D et al., 2007. Supermodeled sabercat, predatory behavior in *Smilodon fatalis* revealed by high-resolution 3D computer simulation. Proc Nat Acad Sin, 104: 16010–16015

Melentis J K, 1968. Die Pikermi fauna von Halmyropotamos (Euböa-Griechenland). Ann Geol Pays Hell, 19: 285–411

Mihlbachler M C, Rivals F, Solounias N et al., 2011. Dietary change and evolution of horses in North America. Science, 331: 1178–1181

Qiu Z X, Huang W L, Guo Z H, 1987. The Chinese hipparionine fossils. Palaeont Sin, New Ser C, 25: 1–243

Qiu Z X, Deng T, Wang B Y, 2004. Early Pleistocene mammalian fauna from Longdan, Dongxiang, Gansu, China. Palaeont Sin, New Ser C, 27: 1–198

Qiu Z X, Shi Q Q, Liu J Y, 2008. Description of skull material of *Machairodus horribilis* Schlosser, 1903. Vert PalAsiat, 46: 265–283

Qiu Z X, Qiu Z D, Deng T et al., 2013. Neogene land mammal stages/ages of China: toward the goal to establish an Asian land mammal stage/age scheme. In: Wang X M, Flynn L J, Fortelius M eds. Fossil Mammals of Asia: Neogene Biostratigraphy and Chronology. New York: Columbia University Press. 29–90

Radloff F G T, du Toit J T, 2004. Large predators and their prey in a southern African savanna: a predator's size determines its prey size range. J Anim Ecol, 73: 410–423

Ronquist F, Teslenko M, van der Mark P et al., 2012. MrBayes 3.2: efficient Bayesian phylogenetic inference and model choice across a large model space. Syst Biol, 61: 539–542

Salesa M J, Antón M, Turner A et al., 2005. Aspects of the functional morphology in the cranial and cervical skeleton of the saber-toothed cat *Paramachairodus ogygia* (Kaup 1832) (Felidae, Machairodontinae) from the Late Miocene of Spain: implications for the origins of the machairodont killing bite. Zool J Linn Soc, 144: 363–377

Spaulding M, Flynn J J, 2012. Phylogeny of the Carnivoramorpha: the impact of postcranial characters. J Syst Palaeont, 10: 653–677

Swofford D L, 1991. PAUP: Phylogenetic Analysis Using. Parsimony, Version 3.1

Turner A, Antón M, 1997. The Big Cats and Their Fossil Relatives. New York: Columbia University Press. 1–234

Van Valkenburgh B, 1988. Incidence of tooth breakage among large, predatory mammals. Am Nat, 131: 291–300

Van Valkenburgh B, 1990. Skeleton and dental predictors of body mass in carnivores. In: Damuth J, MacFadden B J eds. Body Size in Mammalian Paleobiology: Estimation and Biological Implication. Cambridge: Cambridge University Press. 181–205

Van Valkenburgh B, Ruff C B, 1987. Canine tooth strength and killing behaviour in large carnivores. J Zool, 212: 379–397

Van Valkenburgh B, Sacco T, 2002. Sexual dimorphism, social behavior, and intrasexual competition in large Pleistocene carnivorans. J Vert Paleont, 22: 164–169

Werdelin L, 1996. Carnivoran ecomorphology: a phylogenetic perspective. In: Gittleman J L ed. Carnivore Behavior, Ecology, and Evolution, Volume 2. Ithaca: Cornell University Press. 582–624

Wroe S, McHenry C, Thomason J, 2005. Bite club: comparative bite force in big biting mammals and the prediction of predatory behaviour in fossil taxa. Proc R Soc B, 272: 619–625

Xu X, Wang K B, Zhang K et al., 2012. A gigantic feathered dinosaur from the Lower Cretaceous of China. Nature, 484: 92–95

Xue X X, Coombs M C, 1985. A new species of *Chalicotherium* from the Upper Miocene of Gansu Province, China. J Vert Paleont, 5: 336–344

Xue X X, Delson E, 1989. A new species of *Dryopithecus* from Gansu, China. Chin Sci Bull, 34: 223–229

Zhang Y X, Xue X X, 1995. Taphonomy of Longjiagou Hipparionine Fauna (Turolian, Miocene), Wudu County, Gansu Province, China. Beijing: Geological Publishing House. 1–96